Parton Distribution Functions and their applications

Pavel Nadolsky

Department of Physics
Southern Methodist University (Dallas, TX)

Lecture 1
June 19, 2018

The inner world of a hadron

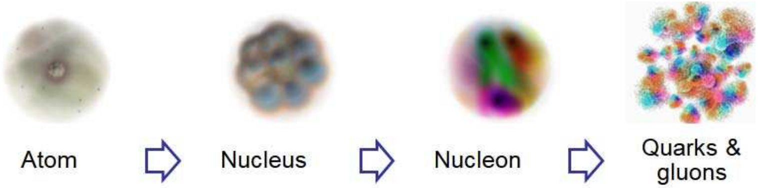

The structure of the hadron drastically changes as the resolution of the “microscope” (scattering process) increases

Parton distributions $f_{a/p}(x,Q)$ characterize the hadronic structure as a function of the energy Q of the hard probe

The inner world of a hadron

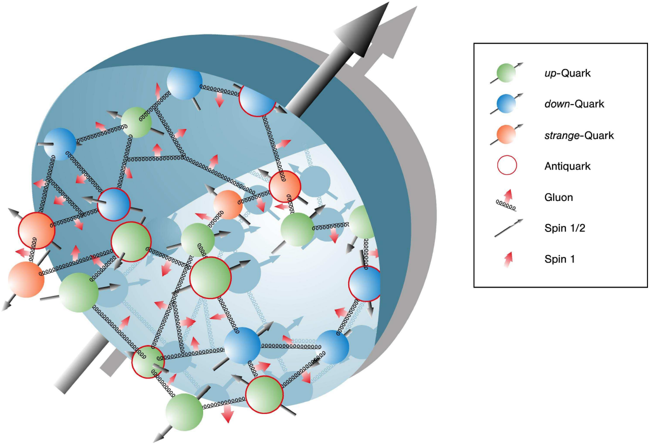

Collinear PDFs $f_{a/p}(x, Q)$ are the simplest among the nonperturbative functions describing the hadron structure. Many considerations here apply to spin-dependent and nuclear PDFs.

Basic definitions

- **Partons** are weakly bound constituents of hadrons with small typical size $(r \ll r_{nucleon} \approx 1\ \text{fm})$

  (Feynman; Bjorken, Paschos - 1969)

  - pointlike, as compared to the "size" of the probe; associated with quantum fields in the SM Lagrangian

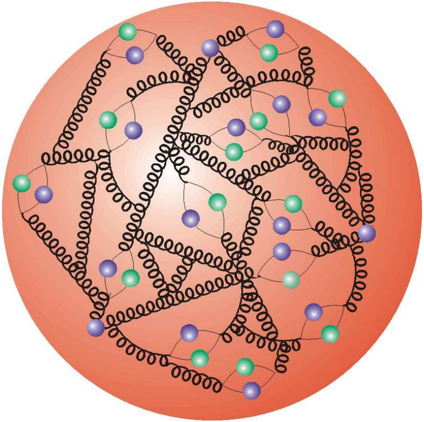

Basic definitions

- Partons are most easily detected in **inclusive** hadronic scattering $A + B \to C + X$ at large collision energy $\sqrt{s} \gg 1$ GeV, with typical energy transfer Q of order $\sqrt{s}$

- Such scattering is dominated by **rare independent collisions** $a + b \to 1 + 2 + ... + n$ of a parton a from A on a parton b from B, proceeding through **perturbative** QCD and electroweak interactions

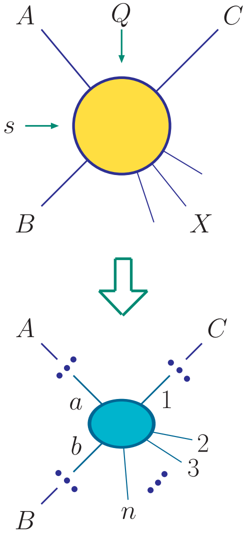

Basic definitions

- In the simplest (leading-order) interpretation, the PDF $f_{a/p}(x,Q)$ is a probability for finding a parton a with 4-momentum xp^α in a proton with 4-momentum p^α
- $f_{a/p}(x,Q)$ depends on **nonperturbative** QCD interactions

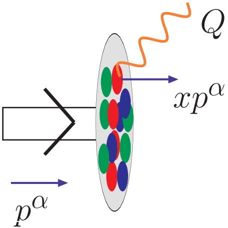

PDFs and QCD factorization

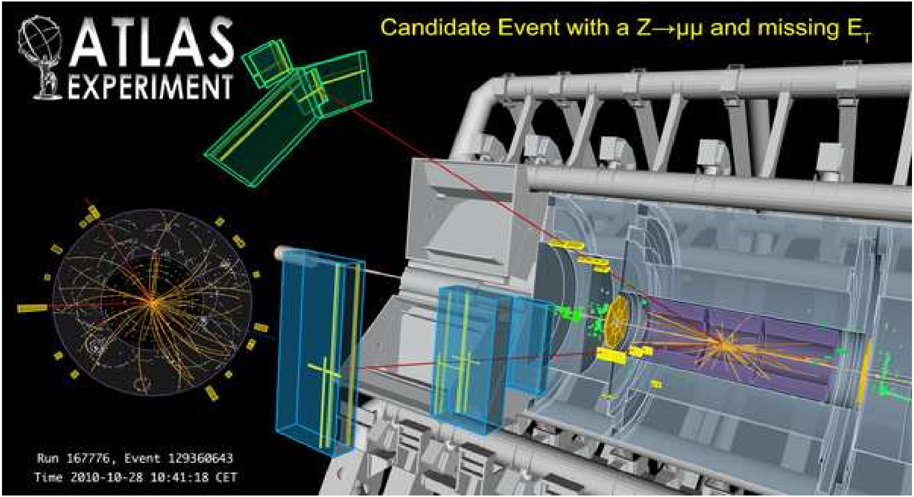

Drell-Yan process $pp \to (Z^0 \to \ell\bar{\ell})X$ at the LHC ($\ell\bar{\ell} = e\bar{e}$ or $\mu\bar{\mu}$)

PDFs and QCD factorization

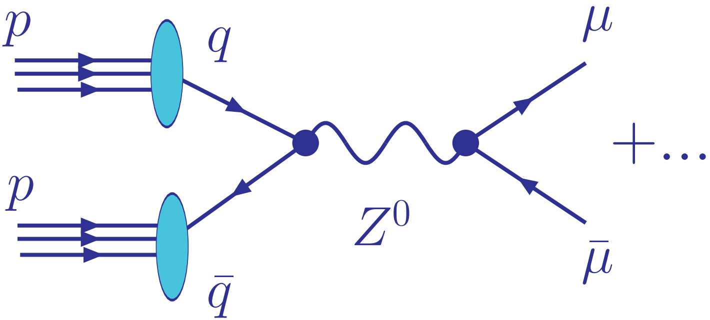

$pp \to (Z^0 \to \mu\bar{\mu})X$: Feynman diagram at the leading order in QCD

PDFs and QCD factorization

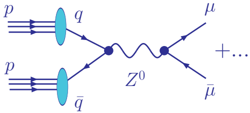

According to QCD factorization theorems, typical cross sections (e.g., for $p(k_1)p(k_2) \to \left[Z(q) \to \ell(k_3)\bar{\ell}(k_4)\right] X$) take the form

$$\sigma_{pp\to\ell\bar{\ell}X} = \sum_{a,b=q,\bar{q},g} \int_0^1 d\xi_1 \int_0^1 d\xi_2\, \widehat{\sigma}_{ab\to Z\to\ell\bar{\ell}} \left(\frac{x_1}{\xi_1}, \frac{x_2}{\xi_2}; \frac{Q}{\mu}\right) f_{a/p}(\xi_1,\mu) f_{b/p}(\xi_2,\mu) + \mathcal{O}\left(\Lambda^2_{QCD}/Q^2\right)$$

- $\widehat{\sigma}_{ab\to Z\to\ell\bar{\ell}}$ is the **hard-scattering cross section**
- $f_{a/p}(\xi,\mu)$ are the **PDFs**
- $Q^2 = (k_3+k_4)^2$, $x_{1,2} = (Q/\sqrt{s})\, e^{\pm y_V}$ — measurable quantities
- ξ_1, ξ_2 are partonic momentum fractions (integrated over)
- μ is a factorization scale (=renormalization scale from now on)

PDFs and QCD factorization

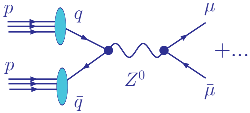

According to QCD factorization theorems, typical cross sections (e.g., for $p(k_1)p(k_2) \to \left[Z(q) \to \ell(k_3)\bar{\ell}(k_4)\right] X$) take the form

$$\sigma_{pp\to\ell\bar{\ell}X} = \sum_{a,b=q,\bar{q},g} \int_0^1 d\xi_1 \int_0^1 d\xi_2\, \widehat{\sigma}_{ab\to Z\to\ell\bar{\ell}}\left(\frac{x_1}{\xi_1}, \frac{x_2}{\xi_2}; \frac{Q}{\mu}\right) f_{a/p}(\xi_1,\mu) f_{b/p}(\xi_2,\mu)$$
$$+\, \mathcal{O}\left(\Lambda^2_{QCD}/Q^2\right)$$

- μ is naturally set to be of order Q
- Factorization holds up to terms of order Λ^2_{QCD}/Q^2

PDFs and QCD factorization

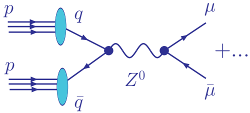

According to QCD factorization theorems, typical cross sections (e.g., for $p(k_1)p(k_2) \to \left[Z(q) \to \ell(k_3)\bar{\ell}(k_4)\right] X$) take the form

$$\sigma_{pp\to\ell\bar{\ell}X} = \sum_{a,b=q,\bar{q},g} \int_0^1 d\xi_1 \int_0^1 d\xi_2\, \widehat{\sigma}_{ab\to Z\to\ell\bar{\ell}}\left(\frac{x_1}{\xi_1}, \frac{x_2}{\xi_2}; \frac{Q}{\mu}\right) f_{a/p}(\xi_1,\mu) f_{b/p}(\xi_2,\mu)$$
$$+ \mathcal{O}\left(\Lambda^2_{QCD}/Q^2\right)$$

Purpose of this arrangement:

- Subtract large collinear logarithms $\alpha_s^n \ln^k(Q^2/m_q^2)$ from $\widehat{\sigma}$
- Resum them in $f_{a/p}(\xi,\mu)$ to all orders of α_s

Operator definitions for PDFs

To all orders in α_s, PDFs are **defined** as matrix elements of certain correlator functions:

$$f_{q/p}(x,\mu) = \frac{1}{4\pi}\int_{-\infty}^{\infty} dy^- e^{iy^- p^+} \langle p \left| \overline{\psi}_q(0, y^-, \vec{0}_T)\gamma^+ \psi_q(0,0,\vec{0}_T) \right| p\rangle, \text{ etc.}$$

Several types of definitions, or **factorization schemes** ($\overline{MS}$, DIS, etc.), exist

They all correspond to the probability density for finding a in p at LO; they differ at NLO and beyond

To prove factorization, one must show that $f_{a/p}(x,\mu)$ correctly captures higher-order contributions for the considered observable

This condition can be violated for multi-scale observables (e.g., DIS or Drell-Yan process at $x \sim Q/\sqrt{s} \ll 1$)

Operator definitions for PDFs

To all orders in α_s, PDFs are **defined** as matrix elements of certain correlator functions:

$$f_{q/p}(x,\mu) = \frac{1}{4\pi}\int_{-\infty}^{\infty} dy^{-} e^{iy^{-}p^{+}} \langle p \left| \overline{\psi}_q(0,y^{-},\vec{0}_T)\gamma^{+}\psi_q(0,0,\vec{0}_T) \right| p\rangle, \text{ etc.}$$

The exact form of $f_{a/p}$ is not known; but its μ dependence is described by **D**okshitzer-**G**ribov-**L**ipatov-**A**ltarelli-**P**arisi (**DGLAP**) equations

$$\mu\frac{df_{i/p}(x,\mu)}{d\mu} = \sum_{j=g,u,\bar{u},d,\bar{d},\dots} \int_x^1 \frac{dy}{y} P_{i/j}\left(\frac{x}{y},\alpha_s(\mu)\right) f_{j/p}(y,\mu)$$

$P_{i/j}$ are probabilities for $j \to ik$ collinear splittings;
are known to order α_s^3 (NNLO):

$$P_{i/j}(x,\alpha_s) = \alpha_s P_{i/j}^{(1)}(x) + \alpha_s^2 P_{i/j}^{(2)}(x) + \alpha_s^3 P_{i/j}^{(3)}(x) + \dots$$

Example of DGLAP evolution

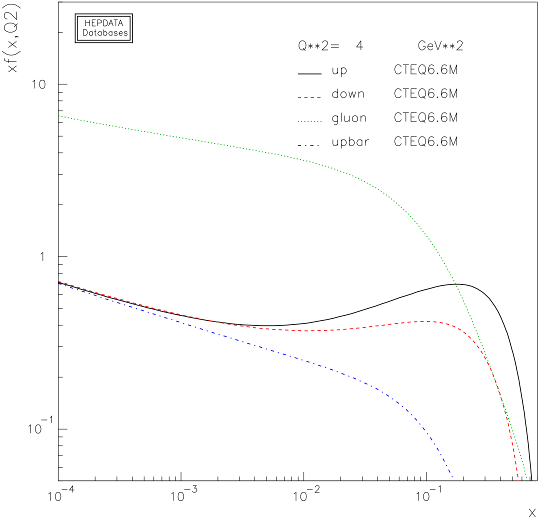

Durham PDF plotter, http://durpdg.dur.ac.uk/hepdata/pdf3.html

Compare μ dependence of u quark PDF and the gluon PDF

The u, d PDFs have a characteristic bump at $x \sim 1/3$ – reminiscent of early valence quark models of the proton structure

The PDFs rise rapidly at $x < 0.1$ as a consequence of perturbative evolution

Example of DGLAP evolution

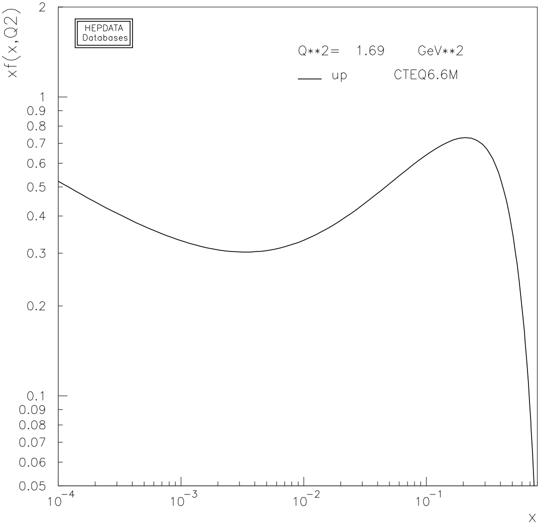

Durham PDF plotter, http://durpdg.dur.ac.uk/hepdata/pdf3.html

As Q increases, it becomes more likely that a high-x parton loses some momentum through QCD radiation

$\Rightarrow u(x, Q)$ reduces at $x \gtrsim 0.1$, increases at $x \lesssim 0.1$

Example of DGLAP evolution

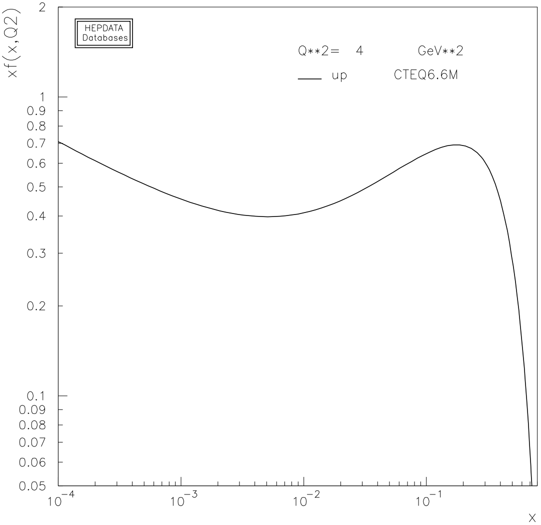

Durham PDF plotter, http://durpdg.dur.ac.uk/hepdata/pdf3.html

As Q increases, it becomes more likely that a high-x parton loses some momentum through QCD radiation

$\Rightarrow u(x,Q)$ reduces at $x \gtrsim 0.1$, increases at $x \lesssim 0.1$

Example of DGLAP evolution

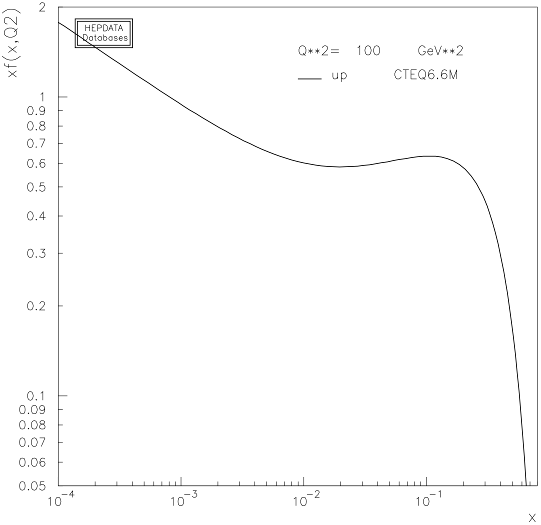

As Q increases, it becomes more likely that a high-x parton loses some momentum through QCD radiation

$\Rightarrow u(x, Q)$ reduces at $x \gtrsim 0.1$, increases at $x \lesssim 0.1$

Durham PDF plotter, http://durpdg.dur.ac.uk/hepdata/pdf3.html

Example of DGLAP evolution

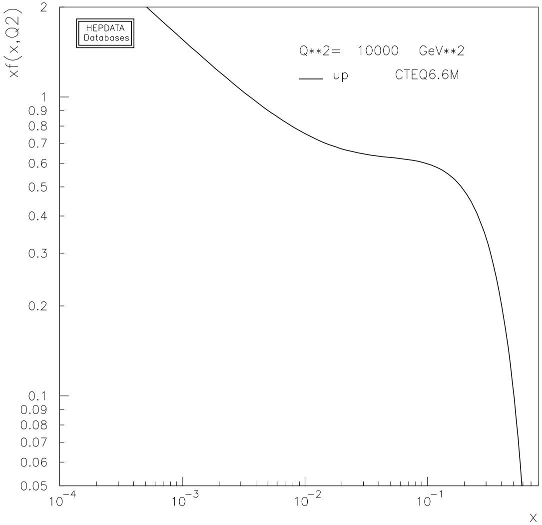

Durham PDF plotter, http://durpdg.dur.ac.uk/hepdata/pdf3.html

As Q increases, it becomes more likely that a high-x parton loses some momentum through QCD radiation

$\Rightarrow u(x,Q)$ reduces at $x \gtrsim 0.1$, increases at $x \lesssim 0.1$

Example of DGLAP evolution: $\bar{u}$ and gluon PDF

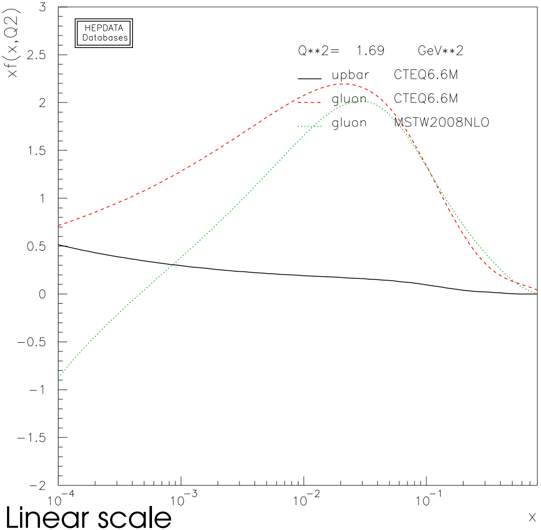

Linear scale

$g(x, Q)$ can become negative at $x < 10^{-2}$, $Q < 2$ GeV

may lead to unphysical predictions

This is an indication that DGLAP factorization experiences difficulties at such small x and Q

Large $\ln^k(1/x)$ in $P_{i/j}(x)$ break PQCD expansion at $x \sim Q/\sqrt{s} \ll 1$

Example of DGLAP evolution: $\bar{u}$ and gluon PDF

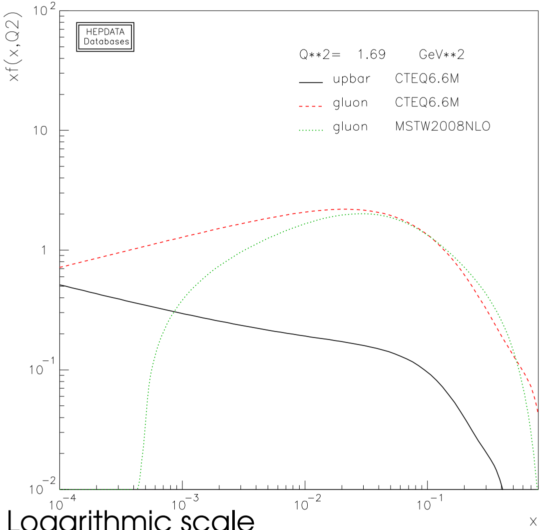

Logarithmic scale

$g(x, Q)$ can become negative at $x < 10^{-2}$, $Q < 2$ GeV

may lead to unphysical predictions

This is an indication that DGLAP factorization experiences difficulties at such small x and Q

Large $\ln^k(1/x)$ in $P_{i/j}(x)$ break PQCD expansion at $x \sim Q/\sqrt{s} \ll 1$

Example of DGLAP evolution: $\bar{u}$ and gluon PDF

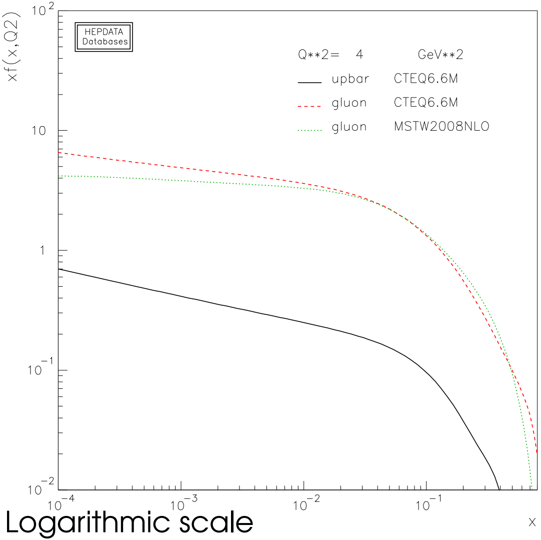

Logarithmic scale

As Q increases, $g(x, Q)$ grows rapidly at small x

$\alpha_s(Q)$ becomes small enough to suppress $\ln^k(1/x)$ terms

small-x behavior stabilizes

Example of DGLAP evolution: $\bar{u}$ and gluon PDF

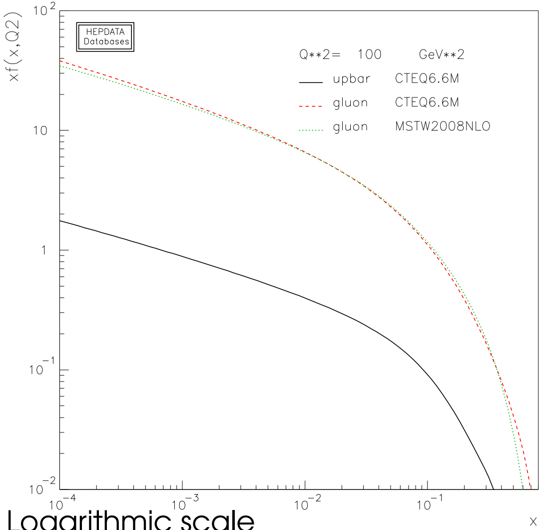

Logarithmic scale

As Q increases, $g(x, Q)$ grows rapidly at small x

$\alpha_s(Q)$ becomes small enough to suppress $\ln^k(1/x)$ terms

small-x behavior stabilizes

Example of DGLAP evolution: $\bar{u}$ and gluon PDF

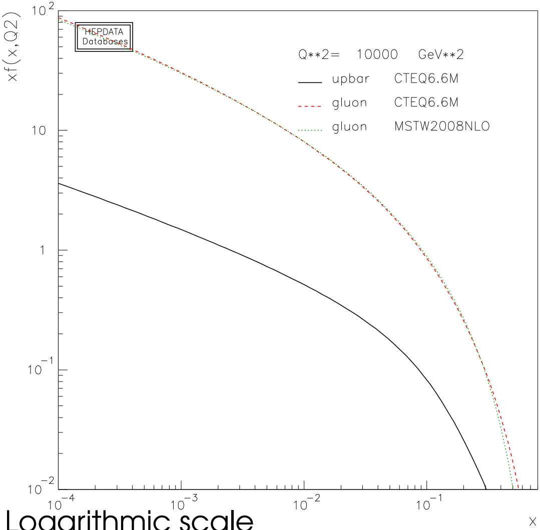

Logarithmic scale

As Q increases, $g(x, Q)$ grows rapidly at small x

$\alpha_s(Q)$ becomes small enough to suppress $\ln^k(1/x)$ terms

small-x behavior stabilizes

Universality of PDFs

To all orders in α_s, PDFs are **defined** as matrix elements of certain correlator functions:

$$f_{q/p}(x,\mu) = \frac{1}{4\pi}\int_{-\infty}^{\infty} dy^- e^{iy^- p^+} \langle p \left| \overline{\psi}_q(0, y^-, \vec{0}_T)\gamma^+ \psi_q(0,0,\vec{0}_T) \right| p\rangle, \text{ etc.}$$

PDFs are **universal** – depend only on the type of the hadron (p) and parton (q, $\bar{q}$, g)

... can be **parametrized** as

$$f_{i/p}(x, Q_0) = a_0 x^{a_1}(1-x)^{a_2} F(a_3, a_4, ...) \text{ at } Q_0 \sim 1 \text{ GeV}$$

... predicted by solving DGLAP equations at $\mu > Q_0$

Factorized QCD predictions

Lepton-hadron scattering

$$\sigma = \sum_a \widehat{\sigma}_a \otimes f_{a/p}$$

Hadron-hadron scattering

$$\sigma = \sum_{a_1, a_2} \widehat{\sigma}_{a_1 a_2} \otimes f_{a_1/p_1} \otimes f_{a_2/p_2}$$

The accuracy in determination of PDFs $f_{a/p}$ must match the accuracy of hard cross sections $\widehat{\sigma}$

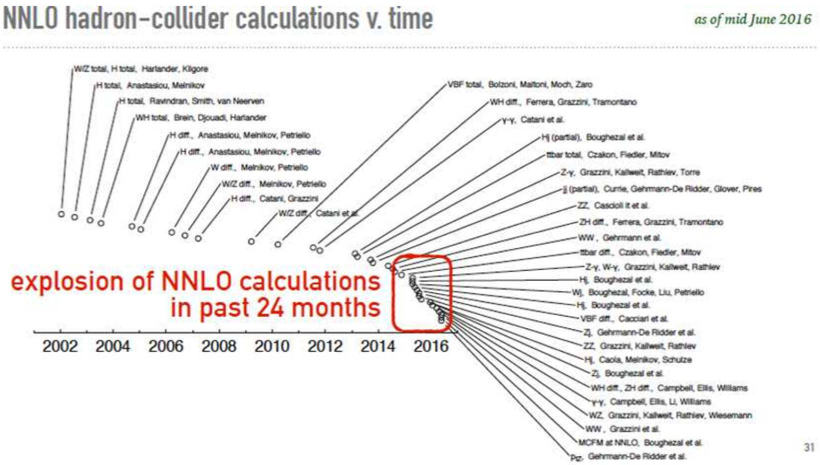

Dramatic advances i n (N)(N)NLO computations in of QCD hard cross sections $\hat{\sigma}$ using automated, recursive, unitarity-based techniques. NNLO hard cross sections $\hat{\sigma}$ accurate to a few percent

Figure by Gavin Salam

General-purpose CT14 PDFs

(S. Dulat et al., arXiv:1506.07443)

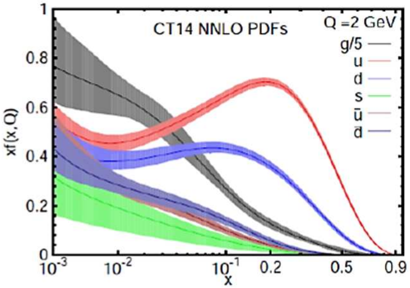

Q= 2 GeV

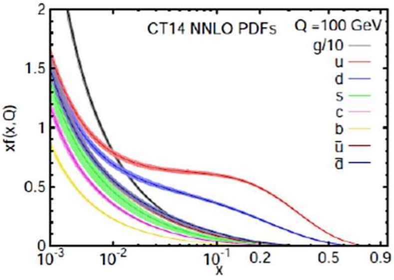

Q= 100 GeV

Phenomenological parametrizations of PDFs are provided with estimated uncertainties of multiple origins (**uncertainties of measurement, theoretical model, parametrization form, statistical analysis**, ...)

The shape of PDFs is optimized w.r.t. hundreds of **nuisance parameters**

Where do the PDFs come from?

Practical answer: from the Les Houches Accord PDF library (LHAPDF)

Almost all recent PDFs are included in the LHAPDF C++ library available at lhapdf.hepforge.org.

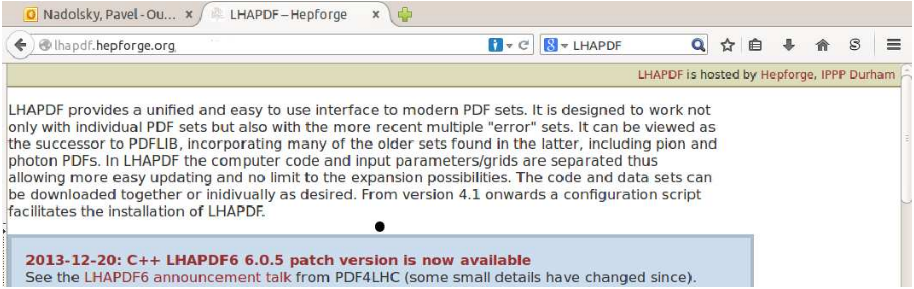

Thousands of PDF sets are provided and can be linked to your computer code. Which one should you use?

Where do the PDFs come from?

- From a combination of **BIG**, medium, and small experiments
- Complementarity in
  - kinematical ranges
  - systematics

+ lattice QCD

The flow of the global analysis

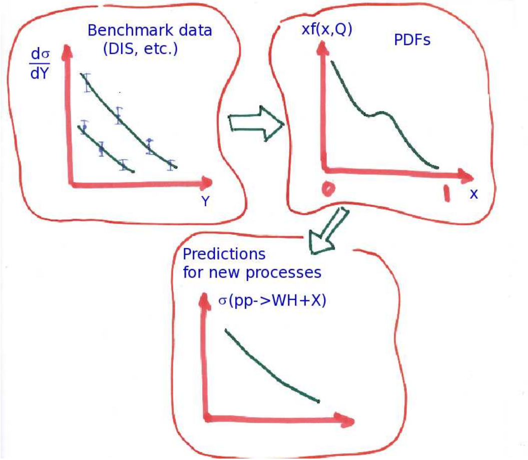

PDFs are not measured directly, but some data sets are sensitive to specific combinations of PDFs. By constraining these combinations, the PDFs can be disentangled in a combined (global) fit.

The flow of the global analysis

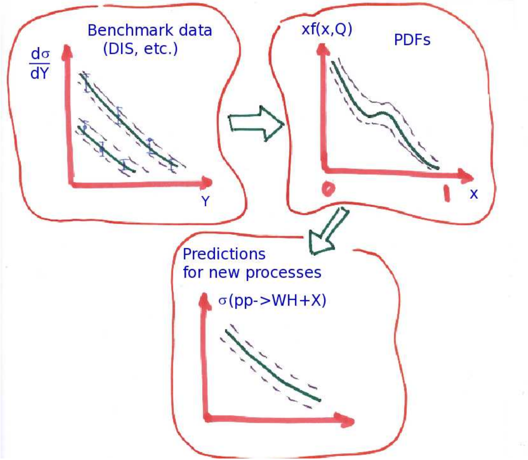

We are interested not just in one best fit, but also in the uncertainty of the resulting PDF parametrizations and theoretical predictions based on them. This will be covered in Lecture 2

Data sets in the CT14 NNLO analysis

S. Dulat et al., arXiv:1506.07443

ID#	Experimental data set		$N_{pt,n}$	χ^2_n
101	BCDMS F_2^p	[24]	337	384
102	BCDMS F_2^d	[25]	250	294
104	NMC F_2^d/F_2^p	[26]	123	133
106	NMC σ^p_{red}	[26]	201	372
108	CDHSW F_2^p	[27]	85	72
109	CDHSW F_3^p	[27]	96	80
110	CCFR F_2^p	[28]	69	70
111	CCFR xF_3^p	[29]	86	31
124	NuTeV $\nu\mu\mu$ SIDIS	[30]	38	24
125	NuTeV $\bar{\nu}\mu\mu$ SIDIS	[30]	33	39
126	CCFR $\nu\mu\mu$ SIDIS	[31]	40	29
127	CCFR $\bar{\nu}\mu\mu$ SIDIS	[31]	38	20
145	H1 σ_r^b	[32]	10	6.8
147	Combined HERA charm production	[33]	47	59
159	HERA1 Combined NC and CC DIS	[34]	579	591
169	H1 F_L	[35]	9	17

ID#	Experimental data set		$N_{pt,n}$	χ^2_n
201	E605 Drell-Yan process	[37]	119	116
203	E866 Drell-Yan process, $\sigma_{pd}/(2\sigma_{pp})$	[38]	15	13
204	E866 Drell-Yan process, $Q^3 d^2\sigma_{pp}/(dQdx_F)$	[39]	184	252
225	CDF Run-1 electron A_{ch}, $p_{T\ell} > 25$ GeV	[40]	11	8.9
227	CDF Run-2 electron A_{ch}, $p_{T\ell} > 25$ GeV	[41]	11	14
234	DØ Run-2 muon A_{ch}, $p_{T\ell} > 20$ GeV	[42]	9	8.3
240	LHCb 7 TeV 35 pb^{-1} W/Z $d\sigma/dy_\ell$	[43]	14	9.9
241	LHCb 7 TeV 35 pb^{-1} A_{ch}, $p_{T\ell} > 20$ GeV	[43]	5	5.3
260	DØ Run-2 Z rapidity	[44]	28	17
261	CDF Run-2 Z rapidity	[45]	29	48
266	CMS 7 TeV 4.7 fb^{-1}, muon A_{ch}, $p_{T\ell} > 35$ GeV	[46]	11	12.1
267	CMS 7 TeV 840 pb^{-1}, electron A_{ch}, $p_{T\ell} > 35$ GeV	[47]	11	10.1
268	ATLAS 7 TeV 35 pb^{-1} W/Z cross sec., A_{ch}	[48]	41	51
281	DØ Run-2 9.7 fb^{-1} electron A_{ch}, $p_{T\ell} > 25$ GeV	[14]	13	35
504	CDF Run-2 inclusive jet production	[49]	72	105
514	DØ Run-2 inclusive jet production	[50]	110	120
535	ATLAS 7 TeV 35 pb^{-1} incl. jet production	[51]	90	50
538	CMS 7 TeV 5 fb^{-1} incl. jet production	[52]	133	177

Modern fits involve up to 40 experiments, $3000+$ data points, and 100+ free parameters

A question to you (think for 1 minute)

Among Standard Model particles, which particles can have a non-zero PDF?

Boundary conditions at $Q_0 \approx 1$ GeV

In practice, independent parametrizations $f_{a/p}(x, Q_0)$ are introduced for

- $g, u, d, s, \bar{u}, \bar{d}, \bar{s}$ (always)
  contribute $> 97\%$ of the proton's energy E_p at Q_0
  - even in this case, the data are usually insufficient for constraining all PDF parameters; some of them can be fixed by hand
  - e.g., $\bar{u} = \bar{d} = \bar{s}$ in outdated fits
- c and or b (occasionally; in a model allowing nonperturbative "intrinsic heavy-quark production")
- photons γ (in QCD+QED PDFs by CT, xFitter, LUX, MRST, NNPDF... groups)

Example: QCD+QED PDFs

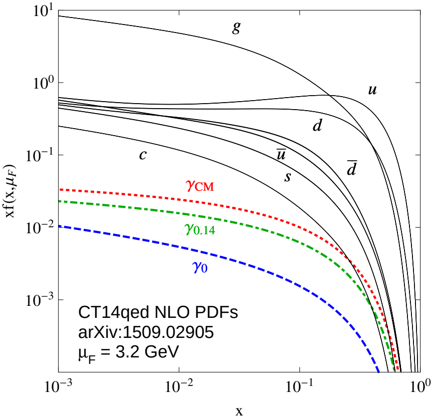

CT14 uses $ep \to e\gamma X$ to constrain $f_{\gamma/p}(x,Q)$

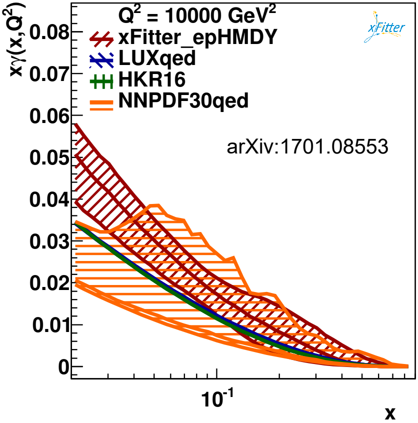

The LUXqed group *(Manohar et al., 1607.04266, 1708.01256)* derives $f_{\gamma/p}(x,Q)$ from DIS inclusive cross section $\Rightarrow$ very small uncertainty on $f_{\gamma/p}(x,Q)$

Another question (1 minute)

Given a QCD observable O, can you tell which parton flavors drive the PDF uncertainty on O? How?

2. Experimental observables constraining the PDFs in global fits

x, Q coverage of various experiments

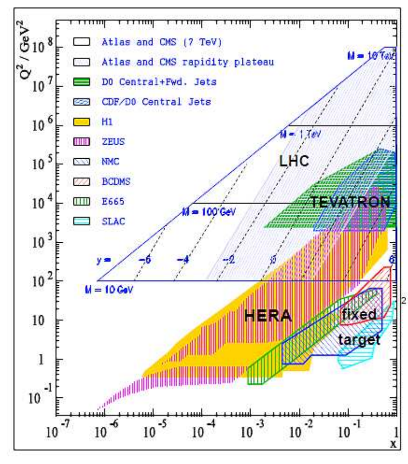

Experiments included in the NNPDF3.1 PDF analysis

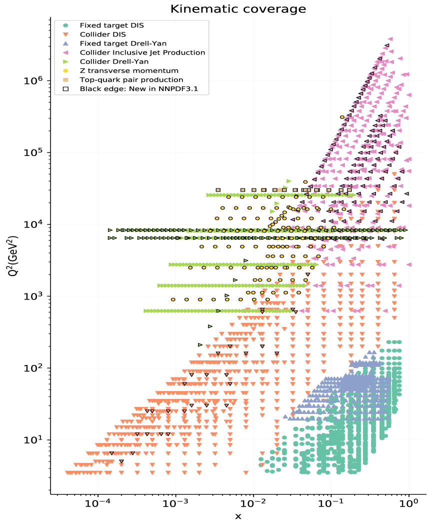

Selection of experimental data for PDF fits (2017)

- **Inclusive deep-inelastic scattering**
  - At HERA:
    neutral-current $e^{\pm}p \to e^{\pm}X$;
    charged-current $ep \to \nu X$
    - the largest data set in the fit
  - Fixed-target experiments
    - eN, μN, νN scattering

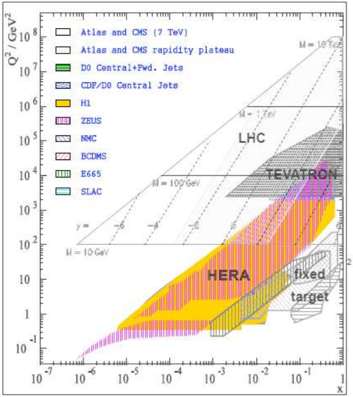

Selection of experimental data for PDF fits (2017)

- **Inclusive deep-inelastic scattering**
  - At HERA:
    neutral-current $e^{\pm}p \to e^{\pm}X$;
    charged-current $ep \to \nu X$
    - the largest data set in the fit
  - Fixed-target experiments
    - $eN, \mu N, \nu N$ scattering

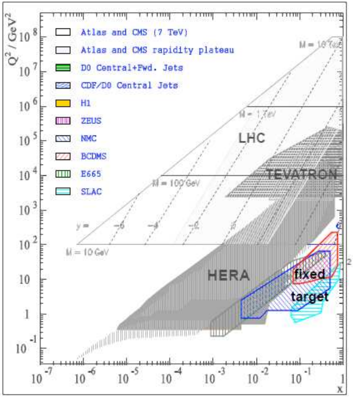

Neutral-current ep DIS: kinematics

- $s = (p_e + p_p)^2$ –total energy
- $Q^2 = -q^2 = -(p_e - p'_e)^2$– momentum transfer
- $x = Q^2/(2p_p \cdot q)$ – Bjorken scaling variable
- $y = Q^2/(xs)$ – inelasticity
- $W^2 = Q^2(1-x)/x$ – energy of the hadronic final state

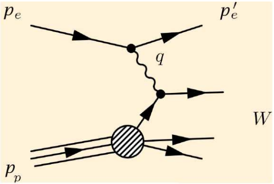

$$\frac{d^2\sigma(e^\pm p)}{dQ^2 dx} = \frac{2\pi\alpha^2}{Q^4 x} Y_+ \left(F_2 - \frac{y^2}{Y_+} F_L \pm \frac{Y_-}{Y_+} x F_3 \right),$$

with $Y_\pm \equiv 1 \pm (1-y)^2$

The data is fitted either in the form of $F_2(x, Q^2)$ or $d^2\sigma/(dQ^2 dx)$

Final combined DIS cross sections at HERA

(arXiv:1506.06042)

41 data sets on NC and CC DIS from H1 and ZEUS are combined into 1 set.

2927 data points are combined into 1307 data points. 165 correlated systematic errors are reanalyzed and calibrated.

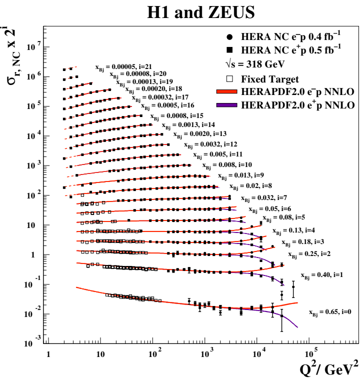

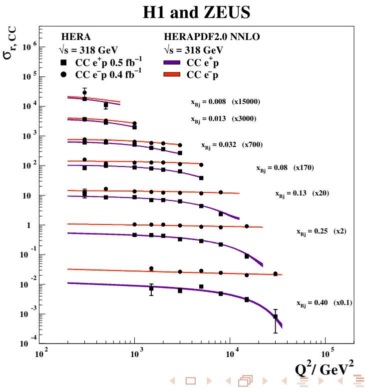

PDF combinations in DIS at the lowest order

- Neutral current $\ell^\pm p$:

$$F_2^{\ell^\pm p}(x,Q^2) = \frac{4}{9}\left(u+\bar{u}+c+\bar{c}\right) + \frac{1}{9}\left(d+\bar{d}+s+\bar{s}+b+\bar{b}\right)$$

  - PDFs are weighted by the fractional EM quark coupling $e_i^2 = 4/9$ or $1/9$
  - 4 times more sensitivity to u and c than to d, s, and b
  - No sensitivity to the gluon at this order

- Neutral current ($\ell^\pm N$) DIS on isoscalar nuclei ($N = (p+n)/2$):

$$F_2^{\ell^\pm N}(x,Q^2) = \frac{5}{9}\left(u+\bar{u}+d+\bar{d}+\text{smaller } s,\ c,\ b \text{ contributions}\right)$$

- Charged current (νN) DIS :

$$F_2^{\nu N}(x,Q^2) = x \sum_{i=u,d,s\ldots} (q_i + \bar{q}_i)$$

$$xF_3^{\nu N}(x,Q^2) = x \sum_{i=u,d,s} (q_i - \bar{q}_i)$$

DIS at next-to-leading order (NLO) and beyond

Logarithmic corrections to Bjorken scaling (Q dependence of $F_2(x, Q^2)$) are sensitive to the gluon PDF through DGLAP equations

Thus, when examined at NLO, the DIS data constrains

- $\sum_i e_i^2(q_i + \bar{q}_i)$ in an amazingly large range $10^{-5} < x < 0.5$
- u and d at $10^{-2} < x < 0.3$
- $g(x, Q)$ at $x < 0.1$

DIS cannot fully separate quarks from antiquarks, or s, c, b contributions from u and d contributions; fixed-target DIS experiments affected by higher-order terms, nuclear corrections,...

Selection of experimental data for PDF fits (2017)

The modern PDF fits include
Inclusive deep-inelastic scattering...

+ Semi-inclusive DIS:

- charm production $ep \to ecX$ (HERA)
- $\mu\mu$ production $\nu N \to \mu(c \to \mu)X$ (NuTeV, NOMAD, ...)

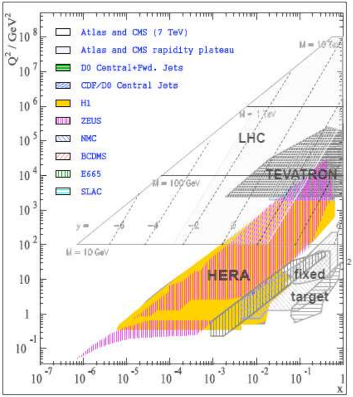

Hard cross sections are known at NNLO (two QCD loops) for inclusive DIS, $ep \to ecX$, $\nu N \to \mu\mu X$

Selection of experimental data for PDF fits (2017)

The modern PDF fits include
Inclusive deep-inelastic scattering...

+ Semi-inclusive DIS:

- charm production $ep \to ecX$ (HERA)
- $\mu\mu$ production $\nu N \to \mu(c \to \mu)X$ (NuTeV, NOMAD, ...)

+ Lepton pair production $pN \overset{\gamma^*,W,Z}{\longrightarrow} \ell\bar{\ell}'X$ (Tevatron, fixed-target experiments)

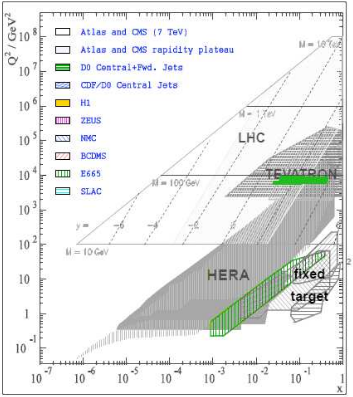

Selection of experimental data for PDF fits (2017)

The modern PDF fits include
Inclusive deep-inelastic scattering...

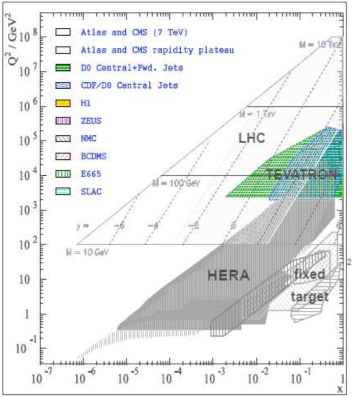

+ Semi-inclusive DIS:

- charm production $ep \to ecX$ (HERA)
- $\mu\mu$ production $\nu N \to \mu(c \to \mu)X$ (NuTeV, NOMAD, ...)

+ Lepton pair production $pN \xrightarrow{\gamma^*, W, Z} \ell\bar{\ell}' X$ (Tevatron, fixed-target experiments)

+ Inclusive jet production: $p\bar{p} \to jX$ (Tevatron), $ep \to j(j)X$ (HERA)

Hard cross sections are known at NNLO (two loops) for lepton pair production, jet, $t\bar{t}$ production

Selection of experimental data for PDF fits (2017)

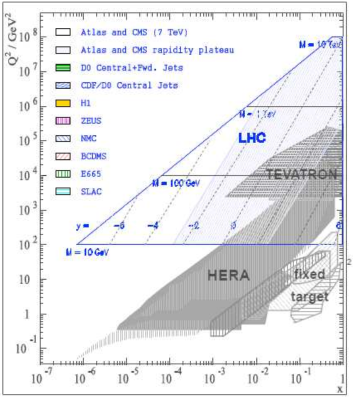

Dozens of data sets from LHC!

- CT14, MMHT14, NNPDF3.0 include early 7 TeV W/Z, jet production data sets
- NNPDF3.1 *(arXiv:1706.00428)* includes high-luminosity data on W/Z, Z p_T, $t\bar{t}$ production
  - moderate reduction in PDF uncertainty, especially for $g(x, Q)$

SU(2) and charge symmetry breaking

$$\bar{d}(x) \neq \bar{u}(x), \quad \bar{q}(x) \neq q(x)$$

May be caused by

- DGLAP evolution
- Fermi motion
- Electromagnetic effects
- Nonperturbative meson fluctuations
- Chiral symmetry breaking
- Instantons
- ...

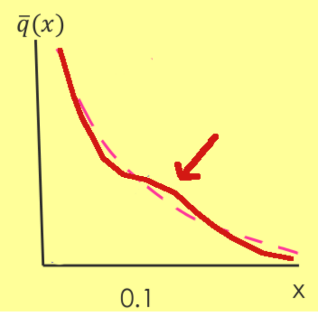

1% accuracy can distinguish between these effects.

Extrinsic and intrinsic sea PDFs

"Extrinsic" sea

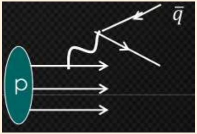

"Intrinsic" sea

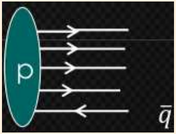

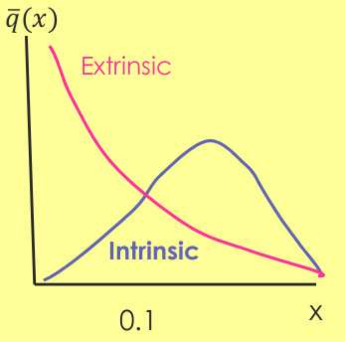

Extrinsic and intrinsic sea PDFs

Smooth $\bar{u}+\bar{d}$ parametrizations can hide existence of two components

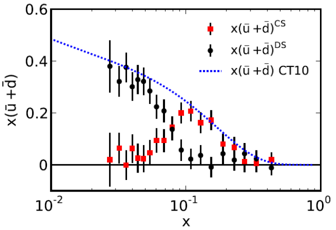

FIG. 5: $x(\bar{u}^{cs}(x)+\bar{d}^{cs}(x))$ obtained from Eq. (1) is plotted together with $x(\bar{u}(x)+\bar{d}(x))$ from CT10 and $\frac{1}{R}x(s(x)+\bar{s}(x))$ which is taken to be $x(\bar{u}^{ds}(x)+\bar{d}^{ds}(x))$.

Liu, Chang, Cheng, Peng, 1206.4339

Intrinsic charm (IC) can carry up to 1% of the proton momentum

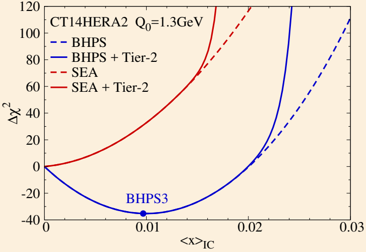

CT14 IC NNLO PDFs
T.-J. Hou et al., 1707.00657

Constraints on quark sea from $pN \to \ell^+\ell^- X$

($N = p,\, d,\, Fe,\, Cu, ..$)

$\frac{d\sigma_{pp}}{dQ^2 dy} \sim (\frac{2}{3})^2 \left[u_A \bar{u}_B + \bar{u}_A u_B\right] + (-\frac{1}{3})^2 \left[d_A \bar{d}_B + \bar{d}_A d_B\right] +$ smaller terms

$\Rightarrow$ sensitivity to $\bar{q}(x,Q)$

Assuming charge symmetry between protons and neutrons ($u_p = d_n,\, u_n = d_p$):

$\frac{d\sigma_{pn}}{dQ^2 dy} \sim (\frac{2}{3})^2 \left[u_A \bar{d}_B + \bar{u}_A d_B\right] + (-\frac{1}{3})^2 \left[d_A \bar{u}_B + \bar{d}_A u_B\right] +$ smaller terms

If deuterium binding corrections are neglected: $q_d(x) \approx q_p(x) + q_n(x)$

At $x_A \gg x_B$ (large y): $\bar{q}(x_A) \sim 0$ and $4u(x_A) \gg d(x_A)$

Constraints on quark sea from $pN \to \ell^+\ell^- X$

($N = p,\ d,\ Fe,\ Cu, ..$)

$$\frac{d\sigma_{pp}}{dQ^2 dy} \sim \left(\frac{2}{3}\right)^2 \left[u_A \bar{u}_B + \bar{u}_A u_B\right] + \left(-\frac{1}{3}\right)^2 \left[d_A \bar{d}_B + \bar{d}_A d_B\right] + \text{ smaller terms}$$

$\Rightarrow$ sensitivity to $\bar{q}(x, Q)$

Assuming charge symmetry between protons and neutrons ($u_p = d_n,\ u_n = d_p$):

$$\frac{d\sigma_{pn}}{dQ^2 dy} \sim \left(\frac{2}{3}\right)^2 \left[u_A \bar{d}_B + \bar{u}_A d_B\right] + \left(-\frac{1}{3}\right)^2 \left[d_A \bar{u}_B + \bar{d}_A u_B\right] + \text{ smaller terms}$$

If deuterium binding corrections are neglected:
$q_d(x) \approx q_p(x) + q_n(x)$

At $x_A \gg x_B$ (large y): $\bar{q}(x_A) \sim 0$ and $4u(x_A) \gg d(x_A)$

Constraints on quark sea from $pN \to \ell^+\ell^- X$ ($N = p,\, d,\, Fe,\, Cu,\, ..$)

$$\frac{d\sigma_{pp}}{dQ^2 dy} \sim \left(\frac{2}{3}\right)^2 \left[u_A \bar{u}_B + \bar{u}_A u_B\right] + \left(-\frac{1}{3}\right)^2 \left[d_A \bar{d}_B + \bar{d}_A d_B\right] + \text{ smaller terms}$$

$\Rightarrow$ sensitivity to $\bar{q}(x, Q)$

Assuming charge symmetry between protons and neutrons ($u_p = d_n,\, u_n = d_p$):

$$\frac{d\sigma_{pn}}{dQ^2 dy} \sim \left(\frac{2}{3}\right)^2 \left[u_A \bar{d}_B + \bar{u}_A d_B\right] + \left(-\frac{1}{3}\right)^2 \left[d_A \bar{u}_B + \bar{d}_A u_B\right] + \text{ smaller terms}$$

If deuterium binding corrections are neglected:

$q_d(x) \approx q_p(x) + q_n(x)$

At $x_A \gg x_B$ (large y): $\bar{q}(x_A) \sim 0$ and $4u(x_A) \gg d(x_A)$

Constraints on quark sea from $pN \to \ell^+\ell^- X$

($N = p,\, d,\, Fe,\, Cu, ..$)

$$\frac{\sigma_{pd}}{2\sigma_{pp}} \approx \frac{1}{2}\frac{(1+\frac{d_A}{4u_A})[1+r]}{(1+\frac{d_A}{4u_A}r)} \approx \frac{1}{2}(1+r),\ \text{where } r \equiv \overline{d}(x_B)/\overline{u}(x_B)$$

$\therefore\ \sigma_{pd}/(2\sigma_{pp})$ constrains $\bar{d}(x,Q)/\bar{u}(x,Q)$ at moderate x

Experimental evidence for SU(2) symmetry breaking

E866 Drell-Yan pair production:
$\bar{d}(x) - \bar{u}(x) \neq 0$ at $x > 0.1$
(large difference)

LHC W/Z production:
$\bar{d}(x) - \bar{u}(x) \neq 0$ at $x < 0.1$
(a few percent)

$\sigma_{pd}/(2\sigma_{pp})$ at large $x_F = x_A - x_B$

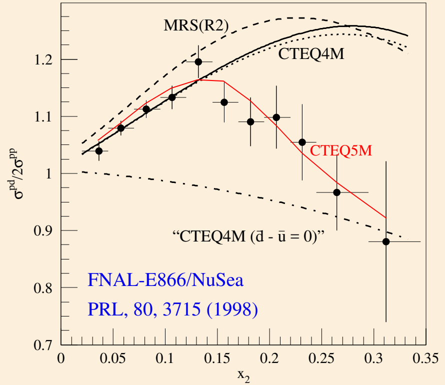

Theory curves reflect different assumptions about $\bar{d}/\bar{u}$

PDF fits (e.g., CTEQ5M) quantitatively account for the violation of $SU(2)$ symmetry in the quark sea

Charged lepton asymmetry in $AB \to (W \to e\nu_e)X$ ($A, B = p$ or $\bar{p}$)

y_e and $\eta \approx y_e$ are rapidity and pseudorapidity of an electron from W decay

$$A_{ch}(y_e) \equiv \frac{\frac{d\sigma^{W^+}}{dy_e} - \frac{d\sigma^{W^-}}{dy_e}}{\frac{d\sigma^{W^+}}{dy_e} + \frac{d\sigma^{W^-}}{dy_e}}$$

$A_{ch}(y_e)$ relates to the boson asymmetry

$A_{ch}(y) = \frac{(d\sigma^{W^+}/dy) - (d\sigma^{W^-}/dy)}{(d\sigma^{W+}/dy) + -(d\sigma^{W^-}/dy)}$, where

$$\left(d\sigma^{W^+}/dy\right) \propto u_A(x_A, M_W)\bar{d}_B(x_B, M_W) + \bar{d}_A(x_A, M_W)u_B(x_B, M_W) + \ldots$$

$$\left(d\sigma^{W^-}/dy\right) \propto \bar{u}_A(x_A, M_W)d_B(x_B, M_W) + d_A(x_A, M_W)\bar{u}_B(x_B, M_W) + \ldots$$

Charged lepton asymmetry in $AB \to (W \to e\nu_e)X$ ($A, B = p$ or $\bar{p}$)

y_e and $\eta \approx y_e$ are rapidity and pseudorapidity of an electron from W decay

$$A_{ch}(y_e) \equiv \frac{\frac{d\sigma^{W^+}}{dy_e} - \frac{d\sigma^{W^-}}{dy_e}}{\frac{d\sigma^{W^+}}{dy_e} + \frac{d\sigma^{W^-}}{dy_e}}$$

$\therefore A_{ch}(y_e)$ constrains PDF ratios at $Q \approx M_W$:

- d/u at $x \to 1$ at the Tevatron 1.96 TeV ($p\bar{p}$);
- d/u at $x > 0.1$ **and** $\bar{u}/\bar{d}$ at $x \sim 0.01$ at the LHC 7 TeV (pp)

Charge asymmetry at the Tevatron and LHC

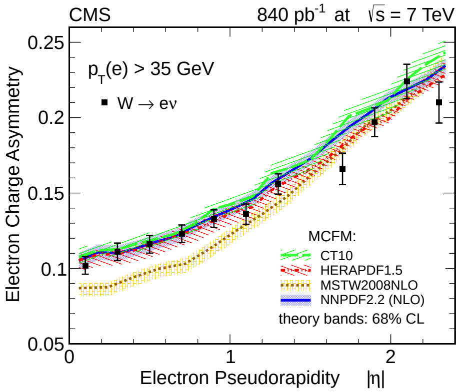

$$A_{ch}(\eta) \equiv \frac{\frac{d\sigma^{W^+}}{d\eta} - \frac{d\sigma^{W^-}}{d\eta}}{\frac{d\sigma^{W^+}}{d\eta} + \frac{d\sigma^{W^-}}{d\eta}}$$

CMS $A_{ch}(\eta)$ data disfavor some d/u parametrizations, motivated an update in MSTW'2008 PDFs

Inclusive jet production, $\overset{(-)}{p p} \to$ jet $+ X$

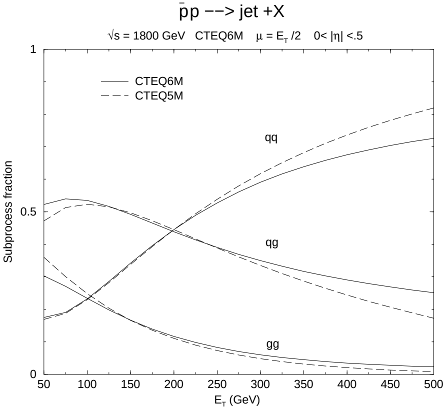

High-E_T jets are mostly produced in qq scattering; yet most of the PDF uncertainty arises from qg and gg contributions

Here typical x is of order $2E_T/\sqrt{s} \gtrsim 0.1$;
e.g., $x \approx 0.2$ for $E_T = 200$ GeV, $\sqrt{s} = 1.8$ TeV

At such x, $u(x,Q)$ and $d(x,Q)$ are known very well; uncertainty arises mostly from $g(x,Q)$

Inclusive jet production in $pp \to$ jet $+X$ (7 TeV)

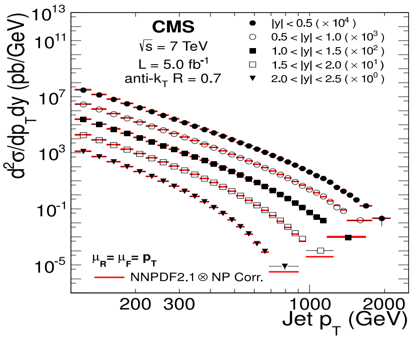

- The cross sections span 12 orders of magnitude
- (Almost) negligible statistical error

Inclusive jet production in $pp \to$ jet $+X$ (7 TeV)

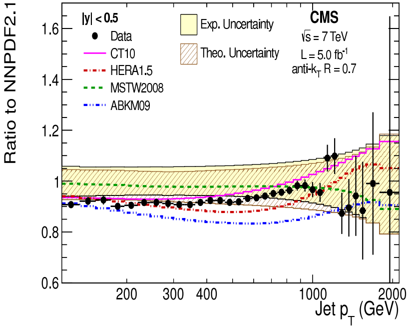

- The cross sections span 12 orders of magnitude
- (Almost) negligible statistical error

- Systematic uncertainties dominate, both from the experiment (up to 90 correlated sources of uncertainty) and NLO theoretical cross section (QCD scale dependence)
- The PDF uncertainty would be strongly underestimated if these systematic errors are not included

Inclusive jet production in $pp \to$ jet $+X$ (7 TeV)

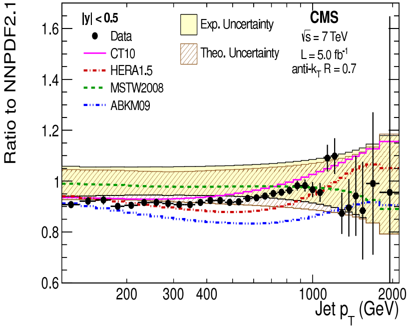

- The cross sections span 12 orders of magnitude
- (Almost) negligible statistical error

- Lecture 2 will discuss how to include the correlated systematic errors into the PDF analysis

Recap, lecture 1

Parton distribution functions $f_{a/p}(x, Q)$...

... are nonperturbative QCD functions describing the structure of hadrons in high-energy scattering according to the method of QCD factorization

... are related to probabilities for finding partons inside parent hadrons

... cannot be computed systematically

... are universal – independent of the hard-scattering process

... obey perturbative evolution (DGLAP) equations

... are determined from select hadronic experiments, used to make predictions for other experiments

Homework assignment

An exotic boson Z' with mass $Q = 2$ TeV is produced similarly to SM Z bosons, but only via the $s\bar{s} \to Z'$ vertex (Z' does not interact with non-strange (anti-)quarks).

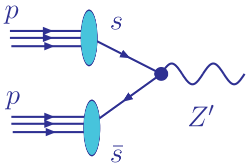

Z'couples only to s,$\bar{s}$

You need to compute $\sigma(pp \to Z'X)$ at the LHC $\sqrt{s} = 13000$ GeV, but for that you need to precisely know the strange (anti-)quark PDFs, $s(x, Q)$ and $\bar{s}(x, Q)$. Propose one or two scattering processes to constrain $s(x, Q)$ and $\bar{s}(x, Q)$ at the relevant $\{x, Q\}$. Specify $\sqrt{s}$ and other kinematic parameters of these processes. Can you use non-LHC measurements to constrain $s(x, Q)$ at the LHC? Why or why not?

3. Choice of PDF parametrization

4. Statistical aspects

5. Practical applications